

Autothermal reforming of CH₄ over supported Ni catalysts prepared from Mg–Al hydrotalcite-like anionic clay

Katsuomi Takehira,^{a,*} Tetsuya Shishido,^a Peng Wang,^b Tokuhiisa Kosaka,^a and Ken Takaki^a

^a Department of Chemistry and Chemical Engineering, Graduate School of Engineering, Hiroshima University, Kagamiyama 1-4-1, Higashi-Hiroshima 739-8527, Japan

^b Japan Science and Technology Corporation, 4-1-8 Honcho, Kawaguchi 332-0012, Japan

Received 21 April 2003; revised 14 July 2003; accepted 21 July 2003

Abstract

spc-Ni/MgAl (spc: solid-phase crystallization method) catalysts have been prepared from Mg–Al hydrotalcite-like compounds containing Ni at the Mg site as the precursors and tested for partial oxidation of CH₄ into synthesis gas. The precursors based on $[\text{Mg}_{1-x}^{2+}\text{Al}_x^{3+}(\text{OH})_2]^{x+}(\text{CO}_3^{2-})_x \cdot m\text{H}_2\text{O}$, in which a ratio of Mg/Al varied and a part of the Mg²⁺ ions were replaced by Ni²⁺ ions, were prepared by a coprecipitation method, thermally decomposed, and reduced to form spc-Ni/MgAl catalyst. Surface areas of spc-Ni/MgAl catalysts were around 150 m² g_{cat}⁻¹. Ni²⁺ ions first substituted a part of the Mg²⁺ sites in the Mg–Al hydrotalcite-like compounds and then incorporated in the rock-salt-type Mg–Ni–O solid solutions in the mixed oxide after the decomposition. The dispersion of Ni was thus repeatedly enhanced during the spc preparation, resulting in the highly dispersed Ni metal particles after the reduction. The activity of the spc-Ni/MgAl catalyst was the highest at the ratio of Mg/Al of 1/3. When the catalysts were tested in the partial oxidation of CH₄, spc-Ni_{0.5}/Mg_{2.5}Al afforded enough high CH₄ conversion even at the high space velocity (9×10^5 ml h⁻¹ g_{cat}⁻¹), exceeding the value obtained over 1 wt% Rh/MgO. Ni species on spc-Ni_{0.5}/Mg_{2.5}Al catalysts were stable even under the presence of O₂, while Ni catalysts prepared by the conventional impregnation quickly lost activity due to the surface oxidation of Ni particles. Moreover, the total heat produced by the reaction was the lowest over the spc-Ni_{0.5}/Mg_{2.5}Al catalyst among the catalysts tested. This strongly suggests that the heat of exothermic CH₄ combustion to H₂O and CO₂ could be quickly consumed by the following endothermic CH₄ reforming by H₂O and CO₂ over spc-Ni_{0.5}/Mg_{2.5}Al. Thus, the spc-Ni_{0.5}/Mg_{2.5}Al catalyst is a hopeful candidate for the autothermal reforming of CH₄ which can be carried out under the copresence of both H₂O and O₂ to feed H₂ to the fuel cell economically. Actually the autothermal reforming of CH₄ has been successfully carried out over spc-Ni_{0.5}/Mg_{2.5}Al catalysts.

© 2003 Elsevier Inc. All rights reserved.

Keywords: Autothermal reforming of CH₄; Solid-phase crystallization method; Supported Ni catalysts; Mg–Al hydrotalcite; High dispersion; Stable Ni metal particles

1. Introduction

Hydrogen production for polymer electrolyte fuel cells (PEFC) is a current topic in the world. Steam reforming of hydrocarbons, especially of methane, is the largest and generally the most economical way to make H₂ [1–3]. An alternative industrial chemical approach includes oxidative reforming of CH₄. However, the H₂ production for PEFC requires enormously high efficiency, taking into account that the reformer should be compact in the FC system not only

on-board a vehicle but also in a stationary FC system. A sufficient amount of H₂ must be continuously produced in a small reformer and fed to the PEFC and, therefore, the reforming catalyst must work under extremely high space velocity. For example, a personal car of 100 horsepower consumes 70 kW of electricity, which requires 70 N m³ h⁻¹ of H₂ for driving, if the PEFC in status quo consumes 1 N m³ h⁻¹ of H₂ for producing 1 kW. Thus, the catalyst for the on-board reformer must be exceptionally active compared with that for Fischer–Tropsch and methanol syntheses. Even in the stationary FC system for home, hospital, and so on, a small reformer is preferable and therefore the catalyst must be highly active. Moreover, the reformer would be frequently started up and shut down during domestic use,

* Corresponding author.

E-mail address: takehira@hiroshima-u.ac.jp (K. Takehira).

and air contamination in the fuel gas could not be avoided. Recently supported precious metal catalysts have frequently been reported to solve these problems [4–11], since the precious metals such as Rh and Ru are highly active and stable for the reforming reactions. However, the cost of the fabrication of the fuel cell system is also important, since a large amount of precious metals is required not only for the reformer but also for the fuel cell. Use of cheaper metals or, at least, a smaller amount of precious metals is preferable for the catalyst preparation of the reformer. These restrictions inevitably require a new concept for the catalyst preparation and also for its use in the reformer.

Supported metal catalysts have been used in the reforming reactions of hydrocarbons and are conventionally prepared by wet impregnation of different supports. This method is not fully reproducible and may give rise to some inhomogeneity in the distribution of the metal on the surface. Moreover, the fine metal particles tend to sinter at high temperature, resulting in the catalyst deactivation. Use of the precursors containing metal ions in the crystal structure, which on further calcination and reduction, may result in the formation of highly dispersed and stable metal particles on the surface. The authors have applied this method for the preparation of stable and highly dispersed metal-supported catalysts as the “solid-phase crystallization” (spc) method and tested it by using perovskite as the precursors [12–15].

The hydrotalcite-like compound is anionic clay, layered mixed hydroxides containing exchangeable anions and produces the oxide by heating that shows interesting properties, such as high surface area, “memory effect,” and basic character [16]. Moreover, upon heating, the compound forms a homogeneous mixture of oxides with very small crystal size, stable against thermal treatments, which by reduction form small and thermally stable metal crystallites. Preparation of heterogeneous catalysts from Mg–Al hydrotalcite-like compounds as the precursors and its utilization for the CH₄ reforming have been claimed [17] and reported by Basini et al. [18,19]. They focused their study on the catalyst application in the CH₄ partial oxidation, and the effects of the residence time and the thermal profile were monitored to know the catalytic reaction mechanism.

We have recently reported that spc-Ni/MgAl catalysts were prepared starting from Mg–Al hydrotalcite-like compounds containing Ni at the Mg sites as the precursors, and were successfully applied for partial oxidation [20], steam reforming [21], and dry reforming of CH₄ [22–25]. It was concluded that the high catalytic performance is uniquely due to the stable and highly dispersed Ni metal particles on the catalysts [26]. In the present paper, we report the effects of Mg/Al ratio and reduction temperature on the Ni dispersion on a spc-Ni/MgAl catalyst, and finally its high activity revealed even at high space velocity in the autothermal reforming of CH₄.

2. Experimental

2.1. Preparation of the catalyst

spc-Ni/MgAl catalysts with various Mg/Al ratios were prepared by the spc method as follows: Mg–Al hydrotalcite precursors based on $[\text{Mg}_{1-x}^{2+}\text{Al}_x^{3+}(\text{OH})_2]^{x+}(\text{CO}_3^{-x}) \cdot m\text{H}_2\text{O}$, in which a part of Mg^{2+} was replaced by Ni^{2+} , were prepared by the coprecipitation method reported by Miyata et al. [27] with minor modifications. The loading amount of Ni was fixed at 16.3 wt% after heating at 1073 K. Both an aqueous solution containing the nitrates of Mg^{2+} , Ni^{2+} , and Al^{3+} and an aqueous solution of sodium hydroxide were added slowly and simultaneously with vigorous stirring into an aqueous solution of sodium carbonate. During the mixing treatment, heavy slurry precipitated. The crystal growth took place by aging the solution at 333 K for 12 h. After the solution was cooled to room temperature, the precipitate was washed with distilled water and dried in air at 353 K. The Mg(Ni)–Al hydrotalcite-like precursors, thus obtained, were heated in a muffle furnace in a static air atmosphere by increasing the temperature from ambient temperature to 1123 K at a rate of 5 K min⁻¹ and kept at 1123 K for 5 h to form the precursor of spc-Ni/MgAl. Surface areas of the precursors of spc-Ni/MgAl catalysts were always high around 150 m² g_{cat}⁻¹. The catalysts were pressed at 25 tons, crushed, and sieved to particles of prescribed size, which were used in the reaction after the prereduction treatment.

As the reference, the catalysts were prepared by conventional impregnation (imp) using $\alpha\text{-Al}_2\text{O}_3$, $\gamma\text{-Al}_2\text{O}_3$, MgO, and Mg–Al mixed oxides prepared from Mg/Al (3/1) hydrotalcite as the carrier. When the Mg–Al mixed oxide was used as the carrier, water or acetone was used as the solvent of $\text{Ni}(\text{NO}_3)_2 \cdot 2\text{H}_2\text{O}$ and the catalyst obtained was denoted as imp-Ni/Mg₃Al-aq or imp-Ni/Mg₃Al-ac. $\text{Ni}(\text{acac})_2$ was also used in acetone solution for impregnation and the catalyst was denoted as imp-Ni/Mg₃Al-acac. The loading amount of Ni was fixed at 16.3 wt% on all the catalysts after the heating.

2.2. Characterization of the catalyst

The structures of the catalysts were studied by XRD, BET, TEM, TPR, and a H₂-adsorption method. X-ray diffraction was measured by using a Rigaku RINT 2550VHF diffractometer with Cu-K α radiation. The diffraction patterns were identified by a comparison with those included in the JCPDS data base (Joint Committee of Powder Diffraction Standards). BET measurements were conducted using N₂ at 77 K with a Bell Japan BELSORP18 instrument. Transmission electron micrographs (TEM) were obtained over on a JEOL JEM3000F instrument equipped with a Hitachi/KeveX H-8100/DeltaIV EDS. Temperature-programmed reduction (TPR) of the catalyst was performed with a U-shaped quartz reactor, the inner diameter of which was 6 mm, at a heating rate of 10 K min⁻¹ using a mixture

of 3 vol% H₂/Ar as reducing gas after passing through a 13X molecular sieve trap to remove water. A TCD was used for monitoring the H₂ consumption. Prior to the TPR measurements, the sample was heated at 573 K for 2 h in 20 vol% O₂/N₂ gas.

The Ni dispersion was determined by static equilibrium adsorption of H₂ at ambient temperature using the pulse method. A 20 mg of the catalyst was prereduced at 1073 K in H₂/N₂ (5/20 ml min⁻¹) flow for 30 min and cooled to ambient temperature in Ar atmosphere. The sample was then used for the measurement by pulsing each 1 ml of 10 vol% H₂/N₂. During the pulse experiment, the amount of H₂ was monitored by a TCD-gas chromatograph. Uptake of H₂ at the monolayer coverage of the Ni species was used to estimate Ni metal dispersion, assuming that each surface Ni site chemisorbs one hydrogen atom (H/Ni_{surface} = 1).

2.3. Catalytic testing

The partial oxidation of CH₄ was conducted using a fixed-bed flow reactor mainly in a mixed gas flow of CH₄, O₂, and N₂ (1/2/1 vol ratio) at 1073 K at atmospheric pressure. The autothermal reforming was carried out mainly in a mixed gas flow of CH₄, O₂, H₂O, and N₂ (2/1/2/1 vol ratio). N₂ gas was used as an internal standard for the analyses by gas chromatography. A U-shaped quartz tube reactor, the inner diameter of which was 6 mm, was used with the catalyst bed near the bottom. The catalyst particles of the size 0.35–0.60-mm diameter were used as dispersed in quartz beads for the space velocity of 4800–290,000 ml h⁻¹ g_{cat}⁻¹. Usually 50 mg of the catalyst was prereduced in a gas flow of 20 vol% H₂/N₂ by increasing the temperature at a rate of 10 K min⁻¹ from ambient temperature to 773 K, followed

by a rate of 2 K min⁻¹ from 773 to 1173 K, and finally by keeping at 1173 for 0.5 h. The thermocouple by which the reaction temperature was controlled was placed at the center of the catalyst bed. Product gases were analyzed by online TCD-gas chromatography. The selectivity to CO₂, CO, or H₂ was calculated based on the numbers of carbon and hydrogen atoms in CH₄. The catalytic activity was also tested by changing the space velocity between 180,000 and 900,000 ml h⁻¹ g_{cat}⁻¹ using 5 mg of the catalyst powders of size less than 0.15 mm ϕ as dispersed in quartz wool.

When the distribution of the temperature in the catalyst bed was measured, 50 mg of the catalyst was dispersed with 500 mg of the quartz beads and packed in the reactor placed across horizontally by using a catalyst holder made by quartz and attached to the thermocouple sheath. The length of the catalyst bed was 18 mm and the temperature was measured by sliding the thermocouple along the catalyst bed.

Also for testing the autothermal reforming of CH₄, O₂, or H₂O was added in the CH₄/H₂O/N₂ or CH₄/O₂/N₂ mixed gas flow, respectively, by changing the flow rate of each gas.

3. Results and discussion

3.1. Preparation of spc-Ni/MgAl catalyst

Metal composition, surface area, Ni dispersion, and size of Ni metal particles of the supported Ni catalysts are shown in Table 1. The composition of metals was determined by ICP analysis for spc-catalysts, while the value was calculated for the imp-catalysts from the amount of raw materials, both after heating at 1123 K. The amount of Ni loading was almost constant around 16 wt% on spc-catalysts. The surface

Table 1
Metal composition, surface area, and Ni dispersion of the catalysts

Catalyst ^a	Atomic ratio (Ni + Mg)/Al	Composition for Al = 1.0 ^b		Ni loading ^b (wt%)	BET surface area ^c (m ² g _{cat} ⁻¹)	H ₂ uptake ^d (μ mol g _{cat} ⁻¹)	Ni dispersion (%)	Particle size of Ni (nm)	
		Ni	Mg					XRD	TEM
spc-Ni _{0.26} /Mg _{0.74} Al	1	0.271	0.703	16.7	124.6	253.5	17.8	7.8	7.0
spc-Ni _{0.38} /Mg _{1.62} Al	2	0.377	1.63	16.0	156.3	247.5	18.2	7.8	6.9
spc-Ni _{0.50} /Mg _{2.50} Al	3	0.488	2.52	15.8	178.6	265.1	19.7	7.0	6.1
spc-Ni _{0.62} /Mg _{3.38} Al	4	0.595	2.90	17.2	141.6	196.0	13.4	8.3	10.2
spc-Ni _{0.73} /Mg _{4.27} Al	5	0.778	3.96	17.8	125.1	203.5	13.4	8.2	12.1
spc-Ni _{0.85} /Mg _{5.15} Al	6	0.824	4.67	16.3	128.5	155.5	11.2	6.6	9.8
imp-Ni/Mg ₃ Al-aq ^e				16.3	95.4	221.5	16.0	7.2	8.3
imp-Ni/Mg ₃ Al-ac ^f				16.3	54.0	66.0	4.8	16.6	22.0
imp-Ni/Mg ₃ Al-acac ^g				16.3	89.2	139.3	10.0	16.7	18.6
imp-Ni/ α -Al ₂ O ₃				16.3	8.2	48.6	3.5	31.1	35.5
imp-Ni/ γ -Al ₂ O ₃				16.3	106.3	122.9	8.9	11.4	13.0
imp-Ni/MgO				16.3	17.2	13.8	1.0	—	8.2

^a Reduced at 1173 K for 0.5 h in H₂/N₂ (5/20 ml min⁻¹).

^b Determined by ICP analysis for spc-catalysts after calcination at 1123 K for 5 h and calculated for imp-catalysts.

^c Calcined at 923 K for 14 h and at 1123 K for 5 h.

^d Determined by H₂ pulse method.

^e Impregnated in aqueous solution of Ni(II) nitrate.

^f Impregnated in acetone solution of Ni(II) nitrate.

^g Impregnated in acetone solution of Ni(II)-acac.

Table 2
Effect of the reduction conditions on the Ni dispersion of the catalysts

Catalyst	Reduction conditions ^a	H ₂ uptake ^b ($\mu\text{mol g}_{\text{cat}}^{-1}$)	Ni dispersion (%)
spc-Ni _{0.5} /Mg _{2.5} Al	1023 K for 0.5 h	83.8	6.2
spc-Ni _{0.5} /Mg _{2.5} Al	1073 K for 0.5 h	221.8	16.5
spc-Ni _{0.5} /Mg _{2.5} Al	1123 K for 0.5 h	244.9	18.2
spc-Ni _{0.5} /Mg _{2.5} Al	1173 K for 0.5 h	265.1	19.7

^a Reduced in H₂/N₂ (5/20 ml min⁻¹).

^b Determined by H₂ pulse method.

area of the catalysts was higher on spc-catalysts than imp-catalysts, the highest value of 178.6 m² g_{cat}⁻¹, among which was obtained with spc-Ni_{0.5}/Mg_{2.5}Al catalysts. Even when Mg₃Al mixed oxide was prepared by heating the hydrotalcite and was used as the support for impregnation, i.e., imp-Ni/Mg₃Al-aq, imp-Ni/Mg₃Al-ac, and imp-Ni/Mg₃Al-acac, the lower values of surface area were obtained compared to the spc-catalysts. Among the other imp-catalysts, imp-Ni/ γ -Al₂O₃ catalyst alone showed a relatively high surface area of 106.3 m² g_{cat}⁻¹. Ni dispersion obtained by H₂ adsorption was also the highest with spc-Ni_{0.5}/Mg_{2.5}Al, followed by the other spc-catalysts. By both increasing and decreasing the Mg/Al ratio, the Ni dispersion decreased. A rather high value of the Ni dispersion was obtained with imp-Ni/Mg₃Al-aq, even though the surface area was not so high, suggesting that Ni was highly dispersed during the preparation (vide infra).

The conditions of the catalyst prereduction affected substantially the Ni metal dispersion (Table 2). Increasing temperatures resulted in higher Ni dispersion as well as the stable activity in the partial oxidation of CH₄ (vide infra). The reduction at 1173 K for 0.5 h afforded the best results and all the catalysts were prereduced under these conditions. Further increase in the reduction temperature or in the reduction time caused the formation of the MgAl₂O₄ spinel phase in the catalyst, resulting in the lowering in the Ni dispersion as well as in the surface area. All catalysts tested for the reforming in this paper were prereduced at 1173 K for 0.5 h.

3.2. Structure of spc-Ni/MgAl catalyst

XRD patterns of spc-Ni/MgAl catalysts during the preparation with various Mg/Al ratios are shown in Fig. 1. In the case of spc-Ni_{0.26}/Mg_{0.74}Al (Mg/Al = 1/1), sharp lines of Al(OH)₃ were observed together with those of Mg–Al hydrotalcite just after the drying of the precipitate. When the Mg/Al ratio was increased above 2/1, no Al(OH)₃ appeared and the hydrotalcite alone was observed after the drying of the precipitate. After the drying, the highest intensity as well as the smallest linewidth in the peaks of the hydrotalcite was observed on spc-Ni/MgAl with the Mg/Al ratio of 2/1–3/1, and both increasing and decreasing Mg/Al ratios caused the line broadening in the hydrotalcite peaks.

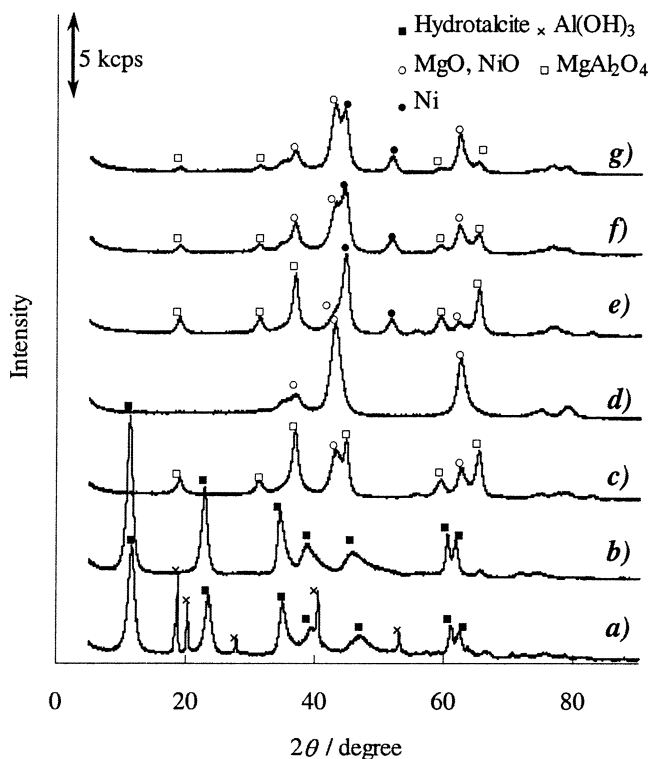


Fig. 1. XRD patterns of the precursors of spc-Ni/MgAl catalysts during the preparation. (a) spc-Ni_{0.26}/Mg_{0.74}Al after drying; (b) spc-Ni_{0.5}/Mg_{2.5}Al after drying; (c) spc-Ni_{0.26}/Mg_{0.74}Al after heating; (d) spc-Ni_{0.5}/Mg_{2.5}Al after heating; (e) spc-Ni_{0.26}/Mg_{0.74}Al after reduction; (f) spc-Ni_{0.38}/Mg_{1.62}Al after reduction; (g) spc-Ni_{0.5}/Mg_{2.5}Al after reduction.

After heating of spc-Ni_{0.26}/Mg_{0.74}Al at 1123 K for 5 h, both the hydrotalcite and the Al(OH)₃ disappeared, and MgO (including Ni as Mg–Ni–O solid solutions) in turn appeared together with MgAl₂O₄ spinel. The line intensities of the MgAl₂O₄ spinel phase were weakened with increasing Mg/Al ratios. The lines of MgO (Mg–Ni–O) were broader in the samples of lower Mg/Al ratios, apparently suggesting that the size of the MgO crystal decreased or the Ni²⁺ incorporation in MgO was enhanced. A lattice constant *a* calculated from the *d* value of MgO (200) plane was smaller than those of MgO and Mg–Ni–O in all spc-Ni/MgAl catalysts, coinciding well with the results reported by Fornasari et al. [28] and Ross [29]. This suggests that Al³⁺, the ionic radii of which (0.54 Å) is smaller than those of Mg²⁺ (0.72 Å) and Ni²⁺ (0.69 Å) [30], was incorporated into MgO to form the solid solutions. Olsbye et al. [31] also reported that Al³⁺ substitutes into the MgO framework and inhibits the crystal growth of MgO in the Mg/Al (3/1) mixed oxide prepared from the hydrotalcite precursor, and a MgAl₂O₄ spinel phase was observed after the steaming test. These coincided well with the results of Al³⁺ incorporation and an excess amount of Al³⁺ was consumed by the formation of the MgAl₂O₄ spinel phase in the present work.

When the sample was reduced in 20 vol% H₂/N₂ at 1173 K, Ni²⁺ in the Mg–Ni–O solid solutions was reduced to form Ni metal. The peaks of Mg–Ni–O were substan-

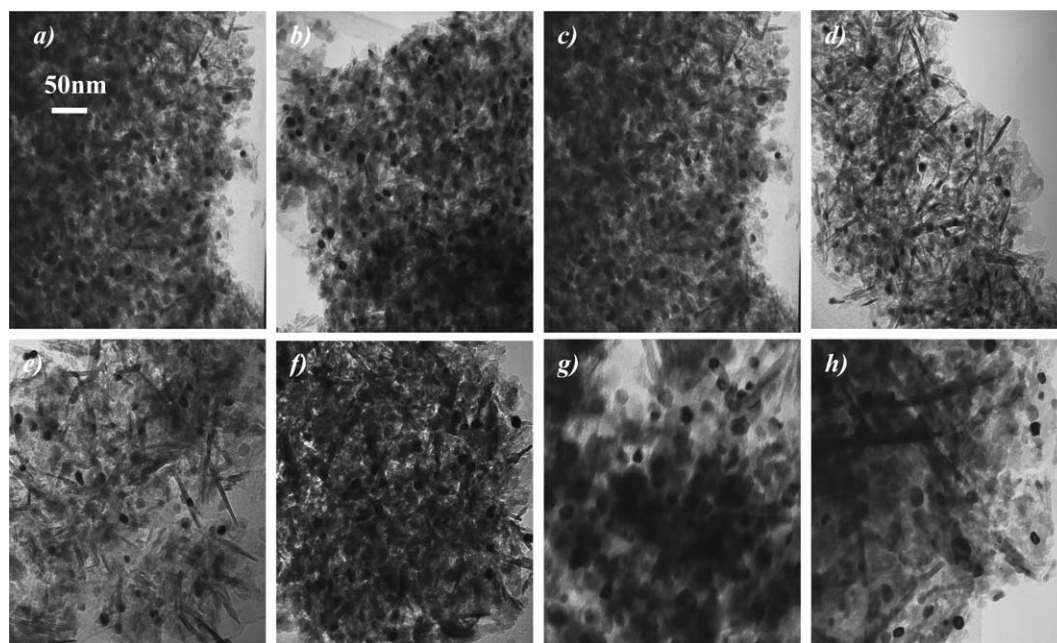


Fig. 2. TEM images of the supported Ni catalysts after reduction. (a) spc-Ni_{0.26}/Mg_{0.74}Al; (b) spc-Ni_{0.32}/Mg_{1.62}Al; (c) spc-Ni_{0.5}/Mg_{2.5}Al; (d) spc-Ni_{0.62}/Mg_{3.38}Al; (e) spc-Ni_{0.73}/Mg_{4.27}Al; (f) spc-Ni_{0.85}/Mg_{5.15}Al; (g) imp-16.3wt%Ni/Mg₃Al-ac; (h) imp-16.3wt%Ni/Mg₃Al-acac.

tially weakened and broadened, while the peaks of Ni metal appeared, with all the catalyst samples. This suggests that, during the release of Ni species from the Mg–Ni–O solid solutions, the MgO crystal structure was collapsed to form the small size particles or amorphous structure. On the other hand, the MgAl₂O₄ spinel phase was still observed after the reduction in the samples of low Mg/Al ratios, probably because this phase does not include Ni²⁺ in the crystal structure.

3.3. Ni dispersion on the catalysts

TEM images of spc-Ni/MgAl catalysts with various Mg/Al ratios after the reduction are shown in Fig. 2, together with those of imp-Ni/Mg₃Al-ac and imp-Ni/Mg₃Al-acac. The average size of Ni metal particles of the catalysts (Table 1) was the smallest with spc-Ni_{0.5}/Mg_{2.5}Al among the spc-catalysts in both TEM images and XRD calculations. Interestingly imp-Ni/Mg₃Al-aq showed a smaller size of Ni metal particles compared to the other imp-catalysts, coinciding well with the results of Ni dispersion (Table 1). Ni metal particles were not clearly observed with imp-Ni/MgO by XRD and Ni dispersion was very low even after the reduction with H₂, suggesting that Ni was stable and hardly reduced in Mg–Ni–O solid solutions. The distributions of the size of Ni metal particles on spc-Ni/MgAl catalysts after the reduction are shown in Fig. 3. The smaller ratio of Mg/Al caused a formation of the smaller size of Ni metal particles after the reduction (Red.) as well as even after the oxidation (POM) of CH₄ for 5 h at 1073 K. After the POM reaction,

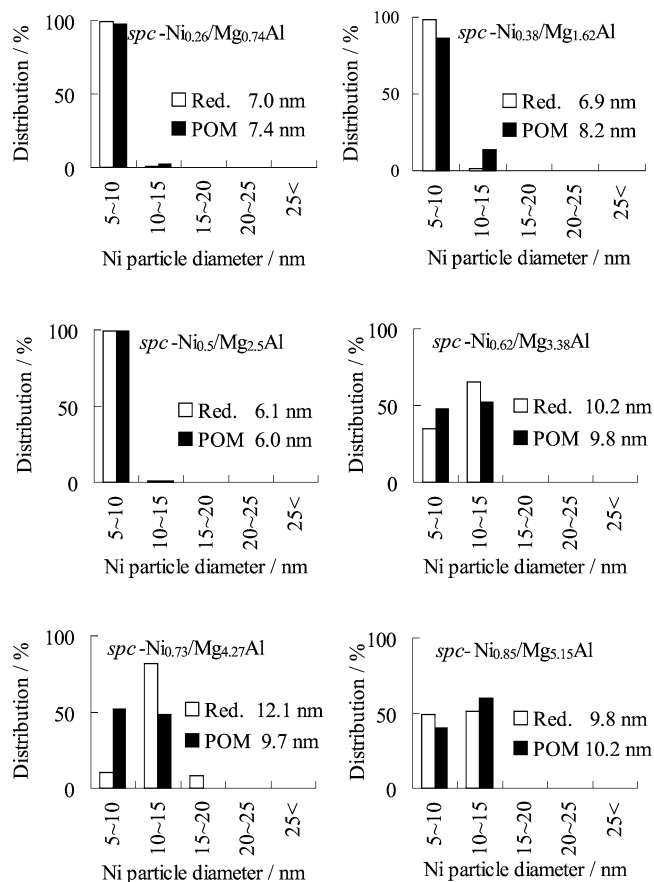


Fig. 3. Distributions of Ni metal particles on spc-Ni/MgAl catalysts. Red., after reduction; POM, after partial oxidation.

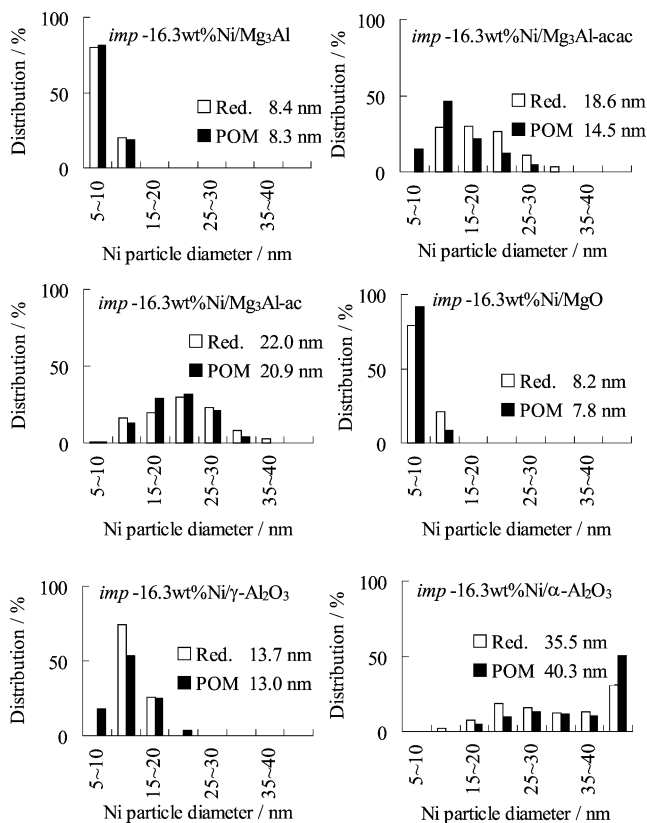


Fig. 4. Distributions of Ni metal particles on imp-Ni catalysts. Red., after reduction; POM, after partial oxidation.

the size of Ni metal particles on both spc-Ni_{0.26}/Mg_{0.74}Al and spc-Ni_{0.38}/Mg_{1.62}Al increased, probably due to the sintering of Ni metal particles during the reaction. On the other hand, when the Mg/Al ratio exceeded 3/1, very interestingly the average size of Ni metal particles rather decreased after the POM reaction except spc-Ni_{0.85}/Mg_{5.15}Al.

The distributions of Ni metal particles on imp-Ni catalysts are shown in Fig. 4. When Ni was loaded on Mg₃Al mixed oxides in aqueous solution, a high dispersion of Ni metal particles was observed as shown in spc-Ni/Mg₃Al-aq. However, use of acetone as the solvent for impregnation resulted in the lower dispersion as shown in both spc-Ni/Mg₃Al-ac and spc-Ni/Mg₃Al-acac. Among both catalysts, a considerably higher dispersion was observed by using Ni(acac)₂ than Ni(NO₃)₂ · 2H₂O. Ni(acac)₂ can form a surface-chelating Ni complex on the catalyst, probably resulting in the high dispersion, while Ni(NO₃)₂ · 2H₂O in acetone cannot afford such an effect. Both imp-Ni/MgO and imp-Ni/γ-Al₂O₃ showed a rather sharp distribution composed of smaller size Ni metal particles compared to those of imp-Ni/α-Al₂O₃. Imp-Ni/MgO and imp-Ni/γ-Al₂O₃ formed Mg–Ni–O solid solutions and NiAl₂O₄ spinel, respectively, also resulting in the high dispersion of Ni metal particles. Moreover, the size of Ni metal particles decreased on spc-Ni/MgAl catalysts as already noted in this paragraph and may be due to the reversible reduction-oxidation of Ni species during the CH₄ oxidation. This reversible reduction-

oxidation between Ni metal and Mg–Ni–O solid solutions may produce finely dispersed Ni metal particles by redistributing Ni species on the catalyst surface.

3.4. TPR of the catalysts

The results of H₂-TPR measurements of spc-Ni/MgAl, together with imp-Ni catalysts as a comparison, are shown in Fig. 5. Obviously Mg₃–Al mixed oxides prepared by heating Mg–Al hydrotalcite showed no reduction peak up to 1300 K. Imp-Ni/γ-Al₂O₃ showed a reduction peak at high temperature, probably due to the formation of NiAl₂O₄ spinel on the catalyst surface. Among imp-Ni/MgAl catalysts, imp-Ni/Mg₃Al-aq showed the highest temperature of the reduction, which is almost the same as that observed with spc-Ni_{0.5}/Mg_{2.5}Al, followed by imp-Ni/Mg₃Al-acac, imp-Ni/Mg₃Al-ac, and imp-Ni/γ-Al₂O₃. During the preparation of imp-Ni/Mg₃Al-aq, surface reconstitution of Mg–Al hydrotalcite possibly took place [16], and Ni was simultaneously incorporated in the hydrotalcite phase, resulting in the highest temperature of the reduction among imp-Ni/MgAl catalysts.

Imp-Ni/MgO showed no peak in the TPR up to 1300 K, while both spc- and imp-Ni/MgAl catalysts showed a clear peak of the Ni reduction. It is likely that Ni²⁺ dissolved in MgO as the solid solutions is not easily reduced to Ni metal, while the addition of Al makes the Ni²⁺ reduction in both imp- and spc-catalysts easy. All spc-Ni/MgAl catalysts showed a reduction peak at high temperatures above 1080 K, and the reduction temperature increased from 1080 to 1190 K with increasing the Mg/Al ratio in

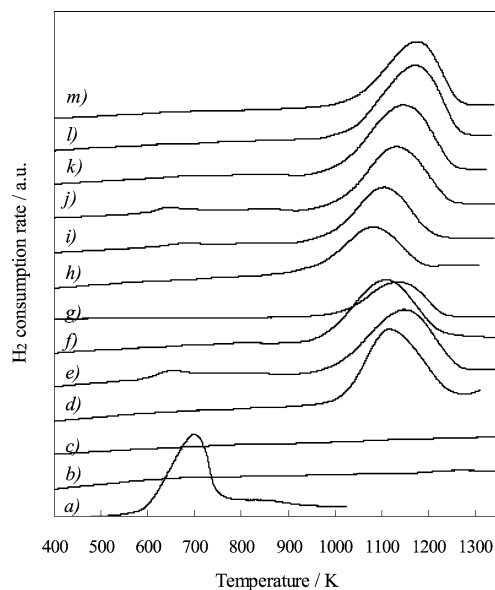


Fig. 5. Temperature-programmed reduction of the supported Ni catalysts. (a) NiO; (b) Mg₃Al mixed oxide; (c) imp-Ni/MgO; (d) imp-Ni/γ-Al₂O₃; (e) imp-16.3wt%Ni/Mg₃Al-acac; (f) imp-16.3wt%Ni/Mg₃Al-ac; (g) imp-16.3wt%Ni/Mg₃Al-aq; (h) spc-Ni_{0.26}/Mg_{0.74}Al; (i) spc-Ni_{0.32}/Mg_{1.62}Al; (j) spc-Ni_{0.5}/Mg_{2.5}Al; (k) spc-Ni_{0.62}/Mg_{3.38}Al; (l) spc-Ni_{0.73}/Mg_{4.27}Al; (m) spc-Ni_{0.85}/Mg_{5.15}Al.

spc-Ni/MgAl catalysts. Judging from the peak area of H₂ consumption, spc-Ni_{0.26}/Mg_{0.74}Al and spc-Ni_{0.38}/Mg_{1.62}Al showed values of 69 and 88%, respectively, of those of the other spc-Ni/MgAl catalysts as the amount of Ni²⁺ reduced in TPR. This means that Ni²⁺ species in both catalysts are not completely reduced. On the other hand, when the Mg/Al ratio exceeded 3/1, the amount of H₂ consumed corresponded well with the amount of Ni²⁺ in each catalyst, suggesting that almost all Ni²⁺ species was reduced in TPR of spc-Ni_{0.5}/Mg_{2.5}Al, spc-Ni_{0.62}/Mg_{3.38}Al, spc-Ni_{0.73}/Mg_{4.27}Al, and spc-Ni_{0.85}/Mg_{5.15}Al.

When the Mg/Al ratio in spc-Ni/MgAl catalysts was increased, the formation of Mg–Ni–O solid solutions might be enhanced under the MgO-rich conditions. This situation leads to an increase in the reduction temperature of Ni. On the contrary, the phase separation into the Mg–Al hydrotalcite and Al(OH)₃ took place after the coprecipitation, followed by the formation of the MgAl₂O₄ spinel phase after heating, in spc-Ni/MgAl catalysts of low Mg/Al ratios. These phenomena may make the catalyst phase more complex, resulting in an easy but incomplete reduction of Ni species in the catalysts.

3.5. Highly dispersed Ni metal particles

On spc-Ni/MgAl catalysts, an increase in the Mg/Al ratio resulted in an increase in the reduction temperature as well as the reduction peak area, suggesting that a large amount of Mg stabilizes a large amount of Ni²⁺ in the solid solutions. Prmaliana et al. [33–36] reported that the MgO–NiO system forms “ideal” solid solutions over the whole molecular fraction range and was used as the catalyst for the steam reforming of CH₄. It is also reported that by Tomishige and co-workers [37–39] that Mg–Ni–O solid solutions of small Ni content showed an excellent stability in dry reforming of CH₄. In the case of Ni catalyst supported on MgO, such treatment, however, leads to the formation of Mg–Ni–O solid solutions. As a result, a considerable amount of Ni diffuses from the catalyst surface into the bulk of the carrier, where it becomes irreducible and therefore ineffective for catalysts [33,36]. An increasing amount of Mg in spc-Ni/MgAl possibly contains an increasing amount of Ni, resulting in a stabilization of Ni species as observed in the increase in the reduction temperature.

On the other hand, Al³⁺ is also incorporated into the MgO framework and inhibits the crystal growth of MgO (probably of Mg–Ni–O solid solutions, too) in the Mg–Al mixed oxide, as noted previously [28,29,31]. This probably makes the Ni reduction in spc-Ni/MgAl catalysts easy. Easy reduction of Ni²⁺ observed in TPR of spc-Ni/MgAl cata-

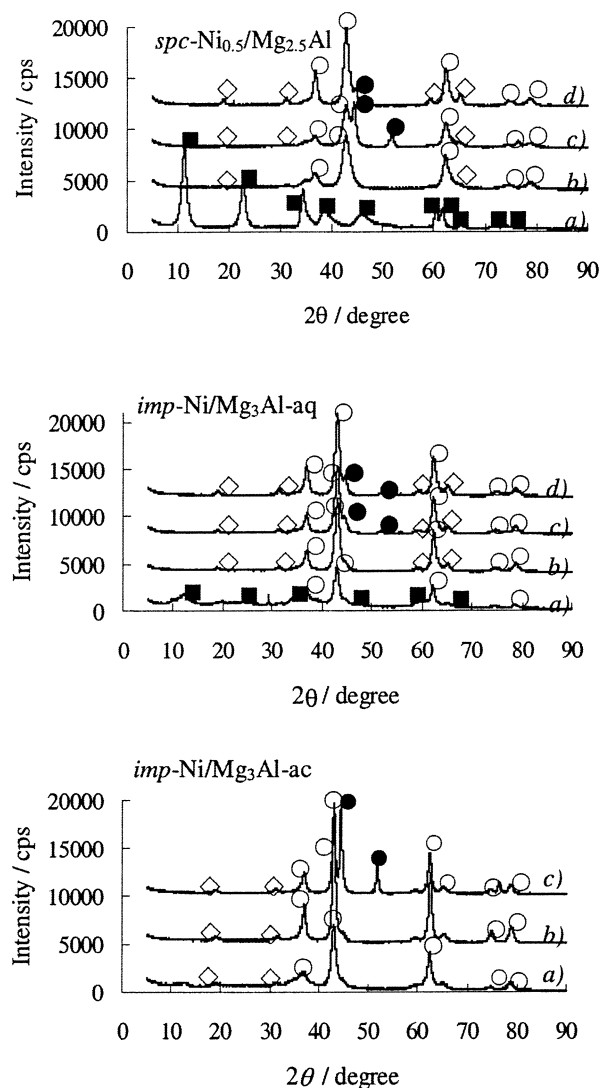


Fig. 6. XRD patterns of supported Ni catalysts. (a) After drying, (b) after heating, (c) after reduction, (d) after reaction (○) Mg–Ni–O; (●): Ni metal; (■): Mg–Al hydrotalcite; (◇): MgAl₂O₄.

lysts is probably due to the substitution of Al³⁺ in MgO which affects the stability of Ni²⁺ in Mg–Ni–O solid solutions. However, the smaller ratio of Mg/Al again resulted in an incomplete reduction of Ni as observed with spc-Ni_{0.26}/Mg_{0.74}Al and spc-Ni_{0.38}/Mg_{1.62}Al (Fig. 5). It is likely that an appropriate value of 3/1 exists in the Mg/Al ratio to reduce efficiently Ni species to form highly dispersed Ni metal particles on spc-Ni/MgAl catalysts.

For imp-Ni/Mg₃Al catalysts, the use of an aqueous solution resulted in the highest reduction temperature, followed by the use of Ni(acac)₂ and Ni(NO₃)₂ · 2H₂O in acetone solution. This may be due to “memory effect” of the hydrotalcite structure [32], i.e., the layered structure of the hydrotalcite was reconstituted, accompanied by the incorporation of Ni at the Mg sites, when Mg₃–Al mixed oxide was immersed in an aqueous solution of Ni(NO₃)₂ · 2H₂O. In fact, the diffraction lines of the hydrotalcite were clearly observed in the XRD results after the impregnation (Fig. 6). It

is expected that the effects of spc preparation also take place on the catalyst surface of imp-Ni/Mg₃Al-aq, resulting in the higher dispersion of Ni metal particles. It is concluded that the reconstitution of the hydrotalcite affords a substantial effect on the formation of highly dispersed Ni metal particles on the supported Ni catalysts prepared by impregnation in aqueous solution. Such effect was not observed when the mixed oxide was dipped in acetone solution as revealed by imp-Ni/Mg₃Al-ac (Fig. 6). An increasing temperature in the reduction peak observed on imp-Ni/Mg₃Al-acac may well coincide with a smaller size of Ni metal particles compared with imp-Ni/Mg₃Al-ac (Table 1 and Figs. 2 and 4). Acetylacetone in Ni(acac)₂ may bind to the catalyst surface and form surface-chelating Ni²⁺acac species, resulting in the formation of smaller size Ni metal particles by inhibiting the cohesion to each other. The largest size of Ni metal particles was obtained over imp-Ni/α-Al₂O₃ as well as the lowest surface area, showing that α-Al₂O₃ is an inert support against Ni (Table 1 and Fig. 4). On the other hand, imp-Ni/γ-Al₂O₃ showed a smaller size of Ni metal particles as well as a reduction peak at the higher temperature compared to imp-Ni/α-Al₂O₃, probably due to the formation of NiAl₂O₄ spinel phase on the catalyst surface. On imp-Ni/α-Al₂O₃, reduction peaks were observed at low temperature almost similar to that on NiO, suggesting that Ni was simply loaded on α-Al₂O₃ without forming any compound.

During the preparation of spc-Ni/MgAl catalysts, Ni was first replaced at the Mg site in Mg–Al hydrotalcite after drying and then incorporated in the rock-salt type Mg–Ni–O solid solutions in the mixed oxide after heating. It is expected that the dispersion of Ni was thus repeatedly enhanced during the spc preparation, resulting in the high dispersion of Ni metal particles after the reduction. It must also be noted that the reducibility of Ni²⁺ in the catalysts was moderately controlled by the incorporation of Al³⁺ in the Mg–Ni–O solid solutions.

3.6. Catalytic behavior of supported Ni catalysts

The catalytic behavior of spc-Ni_{0.5}Mg_{2.5}Al in the partial oxidation of CH₄,



in a CH₄/O₂ = 2/1 mixture was tested on the catalyst by changing the space velocity and compared to the other imp-Ni catalysts (Fig. 7). Dotted lines were obtained by using 50 mg of the catalyst of particle size 0.35–0.60 mm ϕ at a low space velocity, while full lines were obtained with 5 mg of the catalyst powders of the size < 0.15 mm ϕ dispersed in quartz wool at a high space velocity. Generally a higher CH₄ conversion was observed over spc-Ni/MgAl catalysts than imp-catalysts. When space velocity was increased, the Ni catalysts prepared by impregnation of α-Al₂O₃ and MgO, including a commercial Ni/α-Al₂O₃ catalyst, showed clear declines in the CH₄ conversion. On the contrary, spc-Ni_{0.5}Mg_{2.5}Al showed high CH₄ conversion

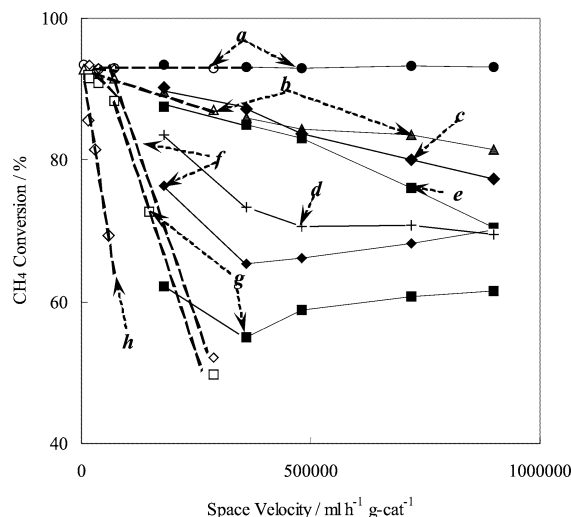


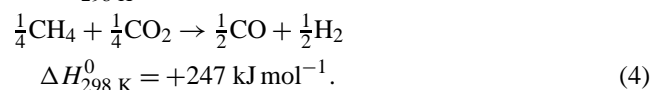
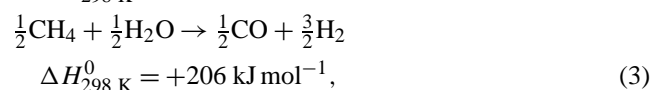
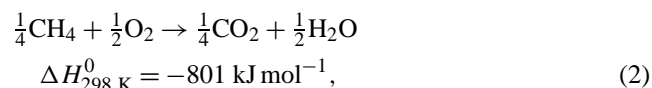
Fig. 7. The partial oxidation of CH₄ over supported Ni catalysts. (a) spc-Ni_{0.5}/Mg_{2.5}Al; (b) imp-16.3wt%Ni/Mg₃Al-aq; (c) imp-16.3wt%Ni/Mg₃Al-acac; (d) imp-16.3wt%Ni/Mg₃Al-ac; (e) imp-16.3wt%Ni/MgO; (f) imp-16.3wt%Ni/γ-Al₂O₃; (g) imp-16.3wt%Ni/α-Al₂O₃; (h) commercial Ni/α-Al₂O₃. A mixed gas of CH₄/O₂/N₂ = 2/1/1 was used at 1073 K for 50 and 5 mg of the catalyst diluted by quartz beads at the low (dotted line) and the high (full line) space velocities, respectively.

even at a high space velocity, followed by imp-Ni/Mg₃Al-aq prepared by impregnation in an aqueous solution of Ni(NO₃)₂ · 2H₂O.

A good performance of imp-Ni/Mg₃Al-aq may be explained by the reconstitution of a hydrotalcite-like structure in aqueous solution during the preparation, resulting in a circumstance around the Ni species in the catalyst partly similar to that of the spc preparation. Imp-Ni/Mg₃Al-acac also showed a good performance with the powdered catalyst, followed by imp-Ni/γ-Al₂O₃, probably due to the high dispersion of Ni metal particles on both catalysts as suggested from the results of TPR. The chelating agent, i.e., acetylacetone, may be effective for dispersing Ni metal particles by binding Ni ions to the catalyst surface. Imp-Ni/Mg₃Al-ac showed rather low CH₄ conversion, and both imp-Ni/MgO and imp-Ni/α-Al₂O₃ showed much lower CH₄ conversion. These may be due to low dispersion (imp-Ni/Mg₃Al-ac and imp-Ni/α-Al₂O₃) or small amount (imp-Ni/MgO) of Ni metal particles on the catalyst surface.

XRD observation of imp-Ni/α-Al₂O₃ after the reaction showed weak diffraction lines due to NiO, suggesting that the surface of Ni metal particles was oxidized during the oxidation. We have observed a similar phenomenon over imp-Ni/SrTiO₃ catalysts during the partial oxidation of CH₄ [15]. When the size of Ni metal particles becomes large on the catalyst, the interaction between metal and support becomes weak, resulting in an easy oxidation of the surface of metal particles during the oxidation reaction. When the space velocity increased, the surface of Ni metal particles can be quickly oxidized, since a large amount of oxygen attacks the catalyst surface and the oxidation reaction proceeds more rapidly than the dissociation of CH₄. The oxidized Ni sur-

face catalyzes the combustion of CH₄ to form CO₂ and H₂O, but does not catalyze the reforming reactions of CH₄ with H₂O and CO₂ to CO and H₂, resulting in a substantial decrease in the CH₄ conversion. The partial oxidation of CH₄ (1) on Ni catalysts is generally composed of an exothermic combustion (2) and two endothermic reforming reactions (3) and (4) under the conditions of CH₄/O₂ = 2/1:



The combustion proceeds more rapidly than the latter two reforming reactions and the rates of the latter reactions considerably depend on the activity of the Ni catalyst used. If the combustion of CH₄ alone takes place over the Ni catalyst, the CH₄ conversion can be calculated as 1/4 = 25% under the gas composition of CH₄/O₂ = 2/1. However, the CH₄ conversion remained at values above 25% over all the powder catalysts tested at the high space velocity. It is likely that certain equilibrium between the oxidized and the reduced states was attained on the surface of Ni particles of the catalyst, and the latter surface still catalyzed the reforming reactions, though poorly, over imp-catalysts.

The behaviors of spc-Ni/MgAl catalysts of various Mg/Al ratios were also tested in the partial oxidation of CH₄ by changing the space velocity (Fig. 8), the highest activity among which was still obtained over spc-Ni_{0.5}/Mg_{2.5}Al with the highest Ni dispersion (Table 1). High activity of spc-Ni_{0.5}/Mg_{2.5}Al proved by the high CH₄ conversion even

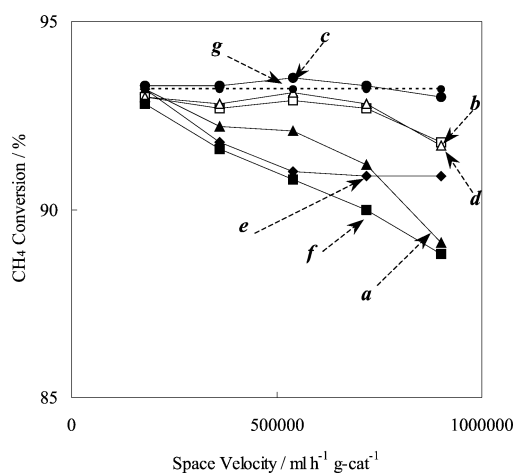


Fig. 8. The partial oxidation of CH₄ over spc-Ni/MgAl catalysts. (a) spc-Ni_{0.26}/Mg_{0.74}Al; (b) spc-Ni_{0.32}/Mg_{1.62}Al; (c) spc-Ni_{0.5}/Mg_{2.5}Al; (d) spc-Ni_{0.62}/Mg_{3.38}Al; (e) spc-Ni_{0.73}/Mg_{4.27}Al; (f) spc-Ni_{0.85}/Mg_{5.15}Al; (g) thermodynamic equilibrium. A mixed gas of CH₄/O₂/N₂ = 2/1/1 was used at 1073 K for 5 mg of the catalyst diluted by quartz beads.

at the high space velocity ($9 \times 10^5 \text{ ml h}^{-1} \text{ g}_{\text{cat}}^{-1}$) corresponds to that of 1 wt% Rh/MgO reported as the best Rh catalyst by Ruckenstein and Wang [4]. Either increasing or decreasing in the Mg/Al ratio from the value of 1/3 resulted in a decrease in the CH₄ conversion with increasing the space velocity. Lower ratios of the Mg/Al, e.g., 1/1, afforded segregation of the Al(OH)₃ phase from Mg–Al hydrotalcite during the co-precipitation, while higher Mg/Al ratio resulted in the formation of a MgO-rich phase after the calcination. The former hindered the formation of a well-crystallized hydrotalcite phase, and the latter strongly held Ni in the MgO structure as the solid solutions by lacking the moderation effects due to the Al³⁺ incorporation. It is likely that both cases suppressed the formation of highly dispersed Ni metal particles, resulting in the lowering of the activity at the high space velocity.

3.7. Temperature of the catalyst bed in partial oxidation of CH₄

When the rates of reforming reactions are slow, the heat of combustion may be accumulated in the catalyst bed, resulting in the formation of a hot spot. On the other hand, if we can provide a catalyst of high performance for the reforming, the heat of combustion may be quickly eliminated from the catalyst bed by the following reforming reactions and therefore no accumulation of the heat appears. The highest temperature was observed at the inlet of the catalyst bed, where the heat accumulation mainly occurred by the combustion. The highest temperatures of the catalyst bed were measured by changing the space velocity from 20,000 to 90,000 ml h⁻¹ g_{cat}⁻¹ on the supported Ni catalysts (Fig. 9). A blank test with quartz wool alone instead of the catalyst afforded a constant temperature covering all the space velocities. Actually less than 5% of CH₄ was consumed by the combustion reaction, resulting in no substantial heat ac-

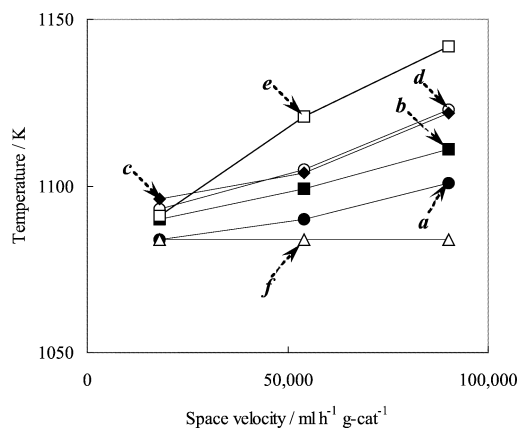


Fig. 9. Temperature at the inlet of the catalyst bed in the partial oxidation of CH₄. (a) spc-Ni_{0.26}/Mg_{0.74}Al; (b) spc-Ni_{0.32}/Mg_{1.62}Al; (c) spc-Ni_{0.5}/Mg_{2.5}Al; (d) spc-Ni_{0.62}/Mg_{3.38}Al; (e) spc-Ni_{0.73}/Mg_{4.27}Al; (f) spc-Ni_{0.85}/Mg_{5.15}Al. A mixed gas of CH₄/O₂/N₂ = 2/1/1 was used at 1073 K for 50 mg of the catalyst diluted by 500 mg of quartz beads. A length of the catalyst bed was 18 mm.

cumulation. Imp-Ni catalysts showed significant increases in the temperature with increasing the space velocity, imp-Ni/ α -Al₂O₃ among which was the highest, followed by imp-Ni/MgO, imp-Ni/ γ -Al₂O₃, and imp-Ni/Mg₃Al-aq. The temperature increase was the smallest with spc-Ni_{0.5}/Mg_{2.5}Al, suggesting that the enhanced endothermic reforming reactions on this catalyst canceled the heat accumulation by the combustion. On the contrary, on imp-Ni/ α -Al₂O₃, the surface of large size Ni metal particles was partially oxidized at the high space velocity, resulting in an enhanced combustion reaction than the reforming reactions followed by the heat accumulation. Imp-Ni/Mg₃Al, imp-Ni/MgO, and imp-Ni/ γ -Al₂O₃ behaved as the catalyst possessing a medium level of activity for the reforming reactions probably depending on each level of Ni metal dispersions. Among these imp-catalysts, imp-Ni/Mg₃Al showed the lowest value of heat accumulation due to the high Ni dispersion accompanied by the reconstitution of Mg–Al hydrotalcite containing Ni during the catalyst preparation. Along the catalyst bed, the temperature decreased from the inlet to the outlet with the all the supported Ni catalysts and showed almost constant temperature around 1090 K at the outlet at the space velocity of 90,000 ml h⁻¹ g_{cat}⁻¹. Only in the case of a blank test, the temperature increased from the inlet (1084 K) to the outlet (1090 K) along the catalyst bed at the same space velocity.

3.8. Autothermal reforming of CH₄

Autothermal reforming of CH₄ was carried out by adding O₂ into the steam reforming mixture of CH₄/H₂O/N₂ = 50/50/100 ml min⁻¹ over 50 mg of the supported Ni catalysts at 1073 K (Fig. 10I). CH₄ conversion calculated by thermodynamic equilibrium increased with increasing the amount of O₂. spc-Ni_{0.5}/Mg_{2.5}Al showed the highest activity in the autothermal reforming of CH₄ almost following the thermodynamic equilibrium, followed by imp-Ni/ γ -Al₂O₃ and imp-Ni/Mg₃Al-aq. Imp-Ni/MgO showed the lowest activity, followed by imp-Ni/ α -Al₂O₃, and both showed decreasing CH₄ conversions by the addition of O₂ at 5 ml min⁻¹.

When the autothermal reforming was carried out by adding H₂O in the partial oxidation mixture of CH₄/O₂/N₂ = 40/20/80 ml min⁻¹, CH₄ conversion at thermodynamic equilibrium increased with increasing the amount of H₂O (Fig. 10II). Twenty-five milligrams of the supported Ni catalysts was used in each reaction. Spc-Ni_{0.5}/Mg_{2.5}Al again showed the highest activity almost following the thermodynamic equilibrium judging from the CH₄ conversion, followed by imp-Ni/ γ -Al₂O₃, imp-Ni/Mg₃Al-aq, and imp-Ni/MgO. The activity of imp-Ni/ α -Al₂O₃ was the lowest, while imp-Ni/MgO showed rather high activity compared to the case of autothermal reforming carried out by adding O₂ to the steam reforming. This may be due to surface oxidation of Ni metal particles on imp-Ni/ α -Al₂O₃. The reaction was carried out by increasing the amount of H₂O in the mixture of CH₄ and O₂, and therefore the surface of Ni metal parti-

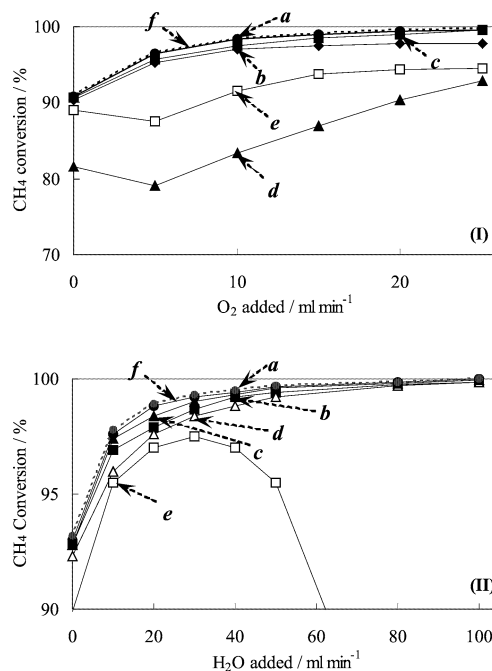


Fig. 10. Autothermal reforming of CH₄ carried out by adding O₂ (I) or H₂O (II) to the steam reforming. (a) spc-Ni_{0.5}/Mg_{2.5}Al; (b) imp-16.3wt%Ni/Mg₃Al-aq; (c) imp-16.3wt%Ni/ γ -Al₂O₃; (d) imp-16.3wt%Ni/MgO; (e) imp-16.3wt%Ni/ α -Al₂O₃; (f) thermodynamic equilibrium. (I) A mixed gas of CH₄/H₂O/N₂ = 50/50/100 ml min⁻¹ was used at 1073 K for 50 mg of the catalyst. (II) A mixed gas of CH₄/O₂/N₂ = 40/20/80 ml min⁻¹ was used for 25 mg of the catalyst.

cles on imp-Ni/ α -Al₂O₃ must be oxidized at the first stage, resulting in a lowering of the activity.

Temperature at the inlet of the catalyst bed increased with increasing the amount of O₂ added in the steam reforming mixture of CH₄/H₂O/N₂ = 50/50/100 ml min⁻¹ (Fig. 11I), showing that endothermic steam reforming was converted to exothermic, i.e., oxidative reforming reaction by the addition of O₂. The reaction temperature was controlled at 1073 K at the center of the catalyst bed. Spc-Ni_{0.5}/Mg_{2.5}Al showed the lowest temperature again as well as no significant increase in the temperature even in the presence of a high amount of O₂, suggesting that the activity for the reforming of this catalyst was the highest among the Ni catalysts tested. Judging from the temperature change, the activity was followed by imp-Ni/ γ -Al₂O₃ and imp-Ni/Mg₃Al-aq. Both imp-Ni/MgO and imp-Ni/ α -Al₂O₃ showed a high temperature of the inlet of the catalyst bed, in which the temperature change was significant with imp-Ni/ α -Al₂O₃. Imp-Ni/ α -Al₂O₃ showed enough high activity in the absence of O₂, while the addition of O₂ (5 ml min⁻¹) caused a clear decrease in the activity (Fig. 10I). This coincided well with the increase in the temperature with the addition of 5 ml min⁻¹ of O₂ (Fig. 11I). The activity of imp-Ni/MgO for steam reforming was very low (Fig. 10I) coinciding well with the high temperature in the absence of O₂ (Fig. 11I).

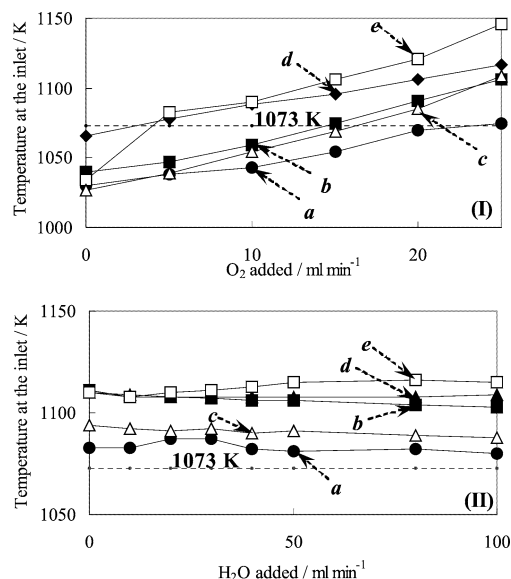


Fig. 11. Temperature at the inlet of the catalyst bed in the autothermal reforming of CH_4 carried out by adding O_2 (I) or H_2O (II). (a) $\text{spc-Ni}_{0.5}/\text{Mg}_{2.5}\text{Al}$; (b) $\text{imp-16.3wt\%Ni}/\text{Mg}_3\text{Al-aq}$; (c) $\text{imp-16.3wt\%Ni}/\gamma\text{-Al}_2\text{O}_3$; (d) $\text{imp-16.3wt\%Ni}/\text{MgO}$; (e) $\text{imp-16.3wt\%Ni}/\alpha\text{-Al}_2\text{O}_3$. (I) A mixed gas of $\text{CH}_4/\text{H}_2\text{O}/\text{N}_2 = 50/50/100 \text{ ml min}^{-1}$ was used at 1073 K for 50 mg of the catalyst. (II) A mixed gas of $\text{CH}_4/\text{O}_2/\text{N}_2 = 40/20/80 \text{ ml min}^{-1}$ was used for 25 mg of the catalyst.

Interestingly, the temperature at the inlet of the catalyst bed did not change significantly when H_2O was added in the partial oxidation mixture of $\text{CH}_4/\text{O}_2/\text{N}_2 = 40/20/80 \text{ ml min}^{-1}$ (Fig. 11II). This may be due to the fact that oxidation proceeds more quickly compared to steam reforming reaction. As a result, the addition of H_2O did not affect substantially the temperature at the inlet of the catalyst bed. $\text{Spc-Ni}_{0.5}/\text{Mg}_{2.5}\text{Al}$ showed again the lowest temperature in the absence of H_2O , followed by $\text{imp-Ni}/\gamma\text{-Al}_2\text{O}_3$, and the temperature gradually decreased with increasing the amount of H_2O added. Also over $\text{imp-Ni}/\text{Mg}_3\text{Al-aq}$ and $\text{imp-Ni}/\text{MgO}$, even though the temperature at the inlet was high, the temperature decreased with increasing the amount of H_2O added, reflecting each activity for the reforming reactions. $\text{Imp-Ni}/\alpha\text{-Al}_2\text{O}_3$ showed a clear increase in the temperature with increasing the amount of H_2O . This may be due to the surface oxidation of Ni metal particles, well coinciding with the low activity (Fig. 10II) as discussed already.

The highest activity was obtained with $\text{spc-Ni}_{0.5}/\text{Mg}_{2.5}\text{Al}$ in both autothermal reforming reactions. A difference in the temperature between the inlet and the outlet of the catalyst bed was $-80, -35, -27, +13, +35,$ and $+47 \text{ K}$, when the amount of O_2 added in the steam reforming over $\text{spc-Ni}_{0.5}/\text{Mg}_{2.5}\text{Al}$ was $0, 5, 10, 15, 20,$ and 25 ml min^{-1} , respectively. The temperature at the inlet of the catalyst bed significantly increased with increasing the amount of O_2 added, clearly showing that endothermic steam reforming was converted to exothermic oxidative reforming. On the other hand, interestingly, the difference in the temperatures

was almost constant as $+38, +32, +32, +34, +37,$ and $+37 \text{ K}$, when the amount of H_2O added was $0, 20, 40, 60, 80,$ and 100 ml min^{-1} , respectively. The reaction was always exothermic and the temperature at the inlet of the catalyst bed was high, showing no substantial effect of H_2O addition in heat production. This may be again due to that the oxidation proceeds faster than the reforming reactions. The distribution of products, i.e., $\text{H}_2, \text{CO},$ and CO_2 as well as CH_4 and H_2O as the raw materials during the reaction over $\text{spc-Ni}_{0.5}/\text{Mg}_{2.5}\text{Al}$ always followed the thermodynamic equilibrium.

3.9. Stability of $\text{spc-Ni}/\text{MgAl}$ catalyst

A long-term stability of $\text{spc-Ni}_{0.5}/\text{Mg}_{2.5}\text{Al}$ was tested in the autothermal reforming of CH_4 at 1073 K for 50 h using 50 mg of the catalyst by feeding the mixed gas of $\text{CH}_4/\text{H}_2\text{O}/\text{O}_2 = 2/2/1$ rather at high GHSV of $1.5 \times 10^5 \text{ ml h}^{-1} \text{ g}_{\text{cat}}^{-1}$ (Fig. 12). The stability of $\text{spc-Ni}_{0.5}/\text{Mg}_{2.5}\text{Al}$ was compared with those of $\text{spc-Ni}_{0.25}/\text{Mg}_{2.75}\text{Al}$, $\text{imp-16.3wt\%Ni}/\text{Mg}_3\text{Al-aq}$, and $\text{imp-8.3wt\%Ni}/\text{Mg}_3\text{Al-aq}$. During the reaction for 50 h, both $\text{spc-Ni}_{0.5}/\text{Mg}_{2.5}\text{Al}$ and $\text{spc-Ni}_{0.25}/\text{Mg}_{2.75}\text{Al}$ showed a quite high stability as well as a high activity, while $\text{imp-16.3wt\%Ni}/\text{Mg}_3\text{Al-aq}$ showed a slow decline and $\text{imp-8.3wt\%Ni}/\text{Mg}_3\text{Al-aq}$ revealed a drastic decrease in the activity after 30 h of the reaction. It is clearly shown that the spc -method afforded a good stability on supported Ni catalysts. Interestingly, even when the loading amount of Ni was decreased to almost half, amount, i.e., 8.3 wt% ($\text{spc-Ni}_{0.25}/\text{Mg}_{2.75}\text{Al}$), the activity was still kept at the same order of $\text{spc-Ni}_{0.5}/\text{Mg}_{2.5}\text{Al}$ during 50 h of the reaction. As shown in Table 2, the condition of prereduction treatment was important for affording the high stability on $\text{spc-Ni}/\text{MgAl}$ catalysts and the reduction at 1173 K for 0.5 h afforded the best results.

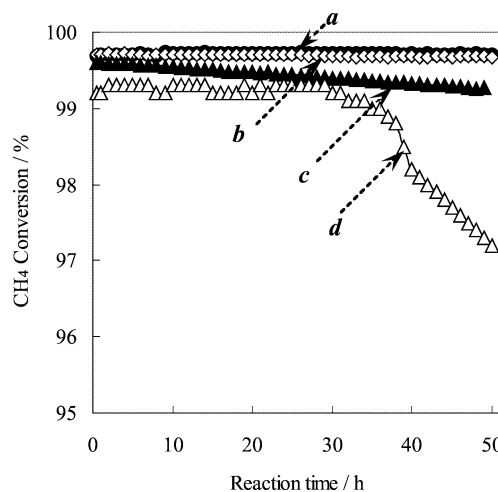


Fig. 12. Autothermal reforming of CH_4 over supported Ni catalysts. (a) $\text{spc-Ni}_{0.5}/\text{Mg}_{2.5}\text{Al}$; (b) $\text{spc-Ni}_{0.25}/\text{Mg}_{2.75}\text{Al}$; (c) $\text{imp-16.3wt\%Ni}/\text{Mg}_3\text{Al-aq}$; (d) $\text{imp-8.3wt\%Ni}/\text{Mg}_3\text{Al-aq}$. A mixed gas of $\text{CH}_4/\text{H}_2\text{O}/\text{O}_2/\text{N}_2 = 50/50/25/25 \text{ ml min}^{-1}$ was used at 1073 K for 50 mg of the catalyst (space velocity = $1.5 \times 10^5 \text{ ml h}^{-1} \text{ g}_{\text{cat}}^{-1}$).

4. Conclusion

spc-Ni/MgAl catalysts have been prepared from Mg–Al hydrotalcite precursors containing Ni at the Mg site and tested for the partial oxidation and autothermal reforming of CH₄ into synthesis gas. The precursors were prepared by the coprecipitation method, thermally decomposed, and reduced to form spc-Ni/MgAl catalysts. Ni²⁺ ions first substituted a part of the Mg²⁺ sites in the Mg–Al hydrotalcite-like compounds, then incorporated in the rock-salt type Mg–Ni–O solid solutions in the mixed oxide after the decomposition, and reduced to be used as the catalysts. The dispersion of Ni was thus repeatedly enhanced during the spc preparation, resulting in the highly dispersed and stable Ni metal particles after the reduction. The activity of spc-Ni/MgAl catalyst was the highest at the ratio of Mg/Al of 1/3. The reducibility of Ni²⁺ was moderately controlled by the Al³⁺ incorporation into the Mg–Ni–O solid solutions. In the partial oxidation of CH₄, spc-Ni_{0.5}/Mg_{2.5}Al afforded enough high CH₄ conversion even at the high space velocity ($9 \times 10^5 \text{ ml h}^{-1} \text{ g}_{\text{cat}}^{-1}$), exceeding the value obtained over 1wt% Rh/MgO. Ni species on spc-Ni_{0.5}/Mg_{2.5}Al catalysts were stable even under the presence of O₂, while Ni catalysts prepared by the conventional impregnation quickly lost activity due to the surface oxidation of Ni particles. Moreover, a heat accumulation during the CH₄ oxidation was the lowest over the spc-Ni_{0.5}/Mg_{2.5}Al catalyst among the catalysts tested. This clearly suggests that the heat of exothermic CH₄ combustion to H₂O and CO₂ could be quickly consumed by the following endothermic CH₄ reforming by H₂O and CO₂ over spc-Ni_{0.5}/Mg_{2.5}Al. Actually spc-Ni_{0.5}/Mg_{2.5}Al showed a high and stable activity for the autothermal reforming of CH₄ under the copresence of O₂ and H₂O. Thus, spc-Ni_{0.5}/Mg_{2.5}Al catalyst is a hopeful candidate for the autothermal reforming of CH₄ which can feed H₂ to fuel cell economically.

Acknowledgments

The authors sincerely thank the Hiroshima Industrial Technology Organization for financial support.

References

- [1] M.A. Pena, J.P. Gomez, J.L.G. Fierro, *Appl. Catal. A* 144 (1996) 7.
- [2] J.N. Armor, *Appl. Catal. A* 176 (1999) 159.
- [3] J.R. Rostrup-Nielsen, *Catal. Today* 71 (2002) 243.
- [4] E. Ruckenstein, H.Y. Wang, *Appl. Catal. A* 198 (2000) 33.
- [5] K. Nakagawa, N. Ikenaga, T. Kobayashi, T. Suzuki, *Catal. Today* 64 (2001) 31.
- [6] F. Basile, G. Fornasari, F. Trifiro, A. Vaccari, *Catal. Today* 64 (2001) 21.
- [7] M.C.J. Bradford, *Catal. Lett.* 66 (2000) 113.
- [8] Y. Schuurman, C. Mirodatos, P. Ferreira-Aparicio, I. Rodriguez-Ramos, A. Guerrero-Ruiz, *Catal. Lett.* 66 (2000) 33.
- [9] P. Pantu, K. Kim, G.R. Gavalas, *Appl. Catal. A* 193 (2000) 203.
- [10] P.M. Tornaiainen, X. Chu, L.D. Schmidt, *J. Catal.* 146 (1994) 1.
- [11] T. Ashcroft, A.K. Cheetham, J.S. Foord, M.L.H. Green, C.P. Grey, A.J. Murrell, P.D.F. Vernon, *Nature* 344 (1990) 319.
- [12] T. Hayakawa, H. Harihara, A.G. Andersen, A.P.E. York, K. Suzuki, H. Yasuda, K. Takehira, *Angew. Chem., Int. Ed. Engl.* 35 (1996) 192.
- [13] A.G. Shiozaki, R. Andersen, T. Hayakawa, S. Hamakawa, K. Suzuki, M. Shimizu, K. Takehira, *J. Chem. Soc., Faraday Trans.* 93 (1997) 3225.
- [14] T. Hayakawa, S. Suzuki, S. Hamakawa, K. Suzuki, T. Shishido, K. Takehira, *Appl. Catal. A* 183 (1999) 273.
- [15] K. Takehira, T. Shishido, M. Kondo, *J. Catal.* 207 (2002) 307.
- [16] F. Cavani, F. Trifiro, A. Vaccari, *Catal. Today* 11 (1991) 173.
- [17] UK Patent 1,442,172, 1973, to BASF AG.
- [18] F. Basile, L. Basini, M. D'Amore, G. Fornasari, A. Guarioni, D. Matteuzzi, G. Del Piero, F. Trifiro, A. Vaccari, *J. Catal.* 173 (1998) 247.
- [19] L. Basini, A. Guarioni, A. Aragano, *J. Catal.* 190 (2000) 284.
- [20] T. Shishido, M. Sukenobu, H. Morioka, M. Kondo, Y. Wang, K. Takaki, K. Takehira, *Appl. Catal. A* 223 (2002) 35.
- [21] P. Shishido, T. Wang, T. Kosaka, K. Takehira, *Chem. Lett.* (2002) 752.
- [22] T. Shishido, M. Sukenobu, H. Morioka, R. Furukawa, H. Shirahase, K. Takehira, *Catal. Lett.* 73 (2001) 21.
- [23] A.I. Tsyganok, K. Suzuki, S. Hamakawa, K. Takehira, T. Hayakawa, *Chem. Lett.* (2001) 24.
- [24] A.I. Tsyganok, K. Suzuki, S. Hamakawa, K. Takehira, T. Hayakawa, *Catal. Lett.* 77 (2001) 75.
- [25] A.I. Tsyganok, T. Tsunoda, K. Suzuki, S. Hamakawa, K. Takehira, T. Hayakawa, *J. Catal.* 213 (2003) 191.
- [26] K. Takehira, *Catal. Surv. Jpn.* 6 (2002) 19.
- [27] M. Miyata, A. Okada, *Clays Clay Miner.* 25 (1977) 14.
- [28] G. Fornasari, M. Gazzano, D. Matteuzzi, F. Trifiro, A. Vaccari, *Appl. Clay Sci.* 10 (1995) 69.
- [29] J.H. Ross, in: G.C. Bond, G. Webb (Eds.), *Specialist Periodical Reports*, Vol. 7, Royal Society Chemistry, London, 1985, p. 1, and references therein.
- [30] R.D. Shannon, *Acta Crystallogr. A* 32 (1976) 751.
- [31] U. Olsbye, D. Akpriaye, E. Rytter, M. Ronnekleiv, E. Tangstad, *Appl. Catal. A* 224 (2002) 39.
- [32] F. Cavani, F. Trifiro, A. Vaccari, *Catal. Today* 11 (1991) 173.
- [33] A. Parmaliana, F. Arena, F. Frusteri, N. Giordano, *J. Chem. Soc., Faraday Trans.* 86 (1990) 2663.
- [34] F. Arena, B.A. Horrell, D.L. Cocke, A. Parmaliana, N. Giordano, *J. Catal.* 132 (1991) 58.
- [35] A. Parmaliana, F. Arena, F. Frusteri, S. Coluccia, L. Marchese, G.L. Martra, A.L. Chuvilin, *J. Catal.* 141 (1993) 34.
- [36] F. Arena, F. Frusteri, A. Parmaliana, L. Plyasova, A.N. Shmakov, *J. Chem. Soc., Faraday Trans.* 92 (1996) 469.
- [37] K. Tomishige, K. Fujimoto, *Catal. Surv. Jpn.* 2 (1998) 3.
- [38] K. Tomishige, Y. Chen, K. Fujimoto, *J. Catal.* 181 (1991) 91.
- [39] Y.-G. Chen, K. Tomishige, K. Yokoyama, K. Fujimoto, *J. Catal.* 184 (1999) 479.
- [40] G.A. Somorjai, *Introduction to Surface Chemistry and Catalysis*, Wiley–Interscience, New York, 1994.